Comparison between the temperature measurements by TIMED/SABER and Lidar in the mid-latitude

Jiyao Xu[1], C. Y. She[2], Wei Yuan[1], Chris Mertens[3], Marty Mlynczak[3], James Russell[4]

1. Laboratory for Space Weather, Center for Space Science and Applied Research, The Chinese Academy of Sciences, China.
2. Department of physics, Colorado State University, Fort Collins, Colorado, USA.
3. NASA/Langley Research Center, Hampton, VA
4. Center for Atmospheric Sciences, Hampton University

Abstract

Comparisons of monthly-mean nighttime temperature profiles observed by the Sodium Lidar at Colorado State University and TIMED/SABER over passes are made. In the altitude range from 85 km to about 100 km, the two observations are in excellent agreement. Though within each other's error bars, important differences occur below 85 km in the entire year and above 100 km in the summer season. Possible reasons for these difference are high photon noise below 85 km in lidar observations, and less than accurate assumptions in the concentration of important chemical species like oxygen (and its quenching rate) in the SABER retrieval above 100 km. However, the two techniques both show the two-level mesopause thermal structure, with the times of change from one level to the other in excellent agreement. Comparison indicates that the high-level (winter) mesopause altitudes are also in excellent agreement between the two observations, though some difference may exist in the low-level (summer) mesopause altitudes between ground-based and satellite-borne data.

Keywords: Atmospheric composition and structure (0300), Pressure, density, and temperature (0350), Middle atmosphere: composition and chemistry (0340), Mesospheric dynamics (3332), Middle atmosphere dynamics (0341, 0342), Remote sensing (3360).

1. Introduction

The temperature profile is one of several very important atmospheric parameters. In the past, it has been difficult to make accurate temperature measurements in the mesosphere and lower thermosphere (MLT) and consequently only a few approaches have been used. These include the falling sphere [Lübken and von Zahn, 1991; Lübken, 1999] and ionization gauge in-situ methods [Fritts, et al., 2004; Lübken and Müllemann, 2003] and the ground-based lidar remote sensing technique. Lidars have the advantage over falling sphere in-situ methods by providing longer-period observations with higher vertical resolution and thus they can observe the temporal evolution of the local atmospheric thermal structure. Sodium lidars have been used routinely to observe the temperature profile in the altitude region from 80 to 105 km [Yu and She, 1995; von Zahn, et al., 1996; Staes and Gardner, 1999].

Satellite remote sensing is the only way to make atmospheric temperature observations on a global scale. The Thermosphere, Ionosphere, Mesosphere, Energetics and Dynamics (TIMED) satellite was launched on December, 7 2001 and carried as one of four experiments, the Sounding of the Atmosphere using Broadband Emission Radiometry (SABER) instrument to remotely sound the temperature distribution from the lower stratosphere to the lower thermosphere, daily and near globally for the first time. SABER also measures O_3, H_2O and CO_2 mixing ratio vertical profiles and key energetics parameters describing upper atmosphere heating, cooling and airglow losses [Russell, et al., 1999]. Temperature is measured using three channels in the 15 μm and 4.3 μm CO2 bands while the remaining seven SABER channels cover the range from 1.27 μm to 9.6 μm.

All emissions observed by SABER are affected by non-local thermal equilibrium (non-LTE) interactions above altitudes of about 75 km. As a result, in order to accurately invert the observed CO_2 emissions to deduce the kinetic temperature, it is necessary to account for non-LTE radiative transfer in the retrieval algorithm [Mertens, et al., 2001; Mertens, et al., 2004]. The effect of non-LTE is also very important for the reduction of atmospheric chemical species [Mertens, et al., 2002; Zhou, et al., 1999; Mlynczak, et al., 1999; Kostov, 1998] and chemical heating and cooling rates [Mlynczak and Solomon, 1993; Fomichev, et al., 1993, 1996; Apruzese, et al., 1984] in the upper mesosphere.

Comparisons between retrieved TIMED/SABER temperature and observations made using other well established methods provide a very good opportunity to assess the extent of our present understanding about non-LTE processes. Mertens et al. [2004] have made comparisons between TIMED/SABER data and rocket falling sphere (FS) measurements in the Arctic summer of 2002. The results indicate that the temperatures observed by SABER and the FS are in good agreement between about 75 and 85 km and between 90 and 97 km.

However, between 85 and 90 km SABER temperatures are significantly different from FS data. The differences may be due to differences in horizontal and temporal resolutions, varying measurement accuracies between the two techniques or they may be the result of the highly variable state of the upper mesosphere. The latter factor may be very important because it is difficult to observe at exactly the same time and in the same sample volume for the satellite and in-situ (and/or ground-based) measurements [Mertens, et al. 2004]. The limb observations for example provide averages over about 300 km distance in the tangent layer along the line-of-sight (LOS) from the satellite to the atmospheric limb whereas the in-situ sensors and lidars make measurements at essentially a single geographic point above the sounding site. While these effects are very important, the full cause for SABER retrieved mesopause altitude at 69^{o}N in the summer to be lower than the FS climatological value [Lübken, 1999] by ~4 km awaits for further study. One phenomenon under investigation is the effect of temperature horizontal gradients that are more severe under polar summer conditions.

In this paper, we make comparisons of monthly-mean profiles between non-LTE retrieved kinetic temperatures from the TIMED/SABER instrument and from the ground-based Na lidar observations in the mid-latitude mesoapuse region for a period of one year (2003). The effect due to differences in temporal and spatial resolution between two instruments should be minimized in monthly-mean, and thus better facilitate comparison. The data sets used and analysis method employed, the results of the comparison, and conclusions will be presented, respectively, in Sections 2, 3 and 4.

2. Data base used and analysis procedure

The altitude of the TIMED orbit is about 625 km. Its inclination is 74.1^{o} from the equator and its orbital period is about 1.6 h. SABER measures the temperature profile from the bottom of the stratosphere to the lower thermosphere. at 15 longitudes each day and on each orbit. Latitude coverage ranges from 54S to 82N or 82S to 54N depending on the TIMED yaw cycle (yawed every 60 days). Since TIMED is a slowly precessing satellite, it takes about 60 days to complete full coverage of 24 hours in local time. To enhance local-time coverage, correlative ground-based observations are of considerable science value. The version 1.04 (level 2A) TIMED/SABER temperature data [http://saber.larc.nasagov/Level2A/] for 2003 are used in this study.

The sodium lidar facility at Colorado State University (41^{o}N, 105^{o}W) was upgraded from a one beam to a two-beam system [She, 2004] in 1999 to prepare for and participate in the correlative CEDAR (Coupling, Energetics, Dynamics of Atmospheric Regions)/TIMED sciences study. The upgraded two-beam system can make simultaneous measurements of mesopause region sodium density, temperature, zonal wind and meridional wind profiles on a 24-hour continuous basis. For the analysis in this paper, we determine hourly-mean temperature

profiles from the averaged simultaneous observations of the two lidar beams. The available hourly-mean temperatures along with horizontal winds for each beam from the CSU lidar, with 2 km vertical resolution at night and 4 km under sunlit condition, may be downloaded from the CEDAR data base [http://cedarweb.hao.ucar.edu/cgi-bin/ion-p?page=cedarweb.ion].

Lidar observations can measure temperature profiles between about 80 and 105 km. As noted earlier, non-LTE processes in this region are very important for the retrieval of kinetic temperature and CO_2 volume mixing ratio from SABER observations. In the nighttime, SABER only observes CO_2 emission in the 15 μm band (not 4.3 μm band); the required CO_2 concentration for kinetic temperature retrieval was obtained from the TIME-GCM (Thermosphere, Ionosphere, Mesosphere and Electrodynamics general circulation model) climatology. It is very difficult to make single profile comparisons (i.e. one SABER profile to one lidar profile) mainly because it is rare if not impossible to achieve complete temporal and spatial coincidence between ground-based and satellite-borne observations. In addition, even though the vertical resolutions of the two techniques are comparable, ~2 km, the horizontal resolutions are very different. The horizontal resolution of SABER is about 300 km along the LOS; in contrast, the two lidar beams are separated by ~70 km with a beam cross-section of only ~100 m. The lidar observations indicate that considerable short wavelength vertical variations exist in the mesopause region temperature profiles due mainly to perturbations caused by atmospheric waves. The satellite observed profiles contain only longer wavelength variations in the vertical temperature profile, because much of the shorter wavelength waves are smoothed out by the horizontal LOS averaging. Furthermore, we note that concentrations of atmospheric chemical species, such as, O_2, N_2, $O(^3P)$ and $O(^1D)$, are required as the input into the non-LTE CO_2 model calculation used in the retrieval algorithm. Among these parameters, the concentration of the atomic oxygen and its quenching rate (k_O) of CO_2 vibrations are most important because of non-radiative collisions with (or quenching of CO_2 vibrations by) atomic oxygen through the process [Mertens, et al., 2001]:

$$CO_2(\nu_2=1) + O \xrightarrow{k_o} CO_2(\nu_2=0) + O. \qquad (1)$$

In the v1.04 SABER temeperature retrievals used in this study, these chemical parameters, such as O_2, N_2, $O(^3P)$ and $O(^1D)$, were obtained from a TIME-GCM modeled climatology [Mertens, et al., 2004.]. The v1.06 temperature retrieval processing currently underway uses $O(^1D)$ determined from $O_2(^1\Delta)$ and OH Meinel band emissions observed by SABER. Model calculations of chemical species represent characteristics of large-scale global distributions. Rocket observations of atomic oxygen indicate that the density of the atomic oxygen was often significantly perturbed by the passage of an atmospheric gravity wave or tide, and by the subsequent convective or dynamical instabilities induced by superposition of that wave [Iwagami, et al., 2003; Howlett, et al., 1980; Melo, et

al., 1996; Hecht, et al., 2004]. So, the density of atomic oxygen used in the temperature retrieval can be quite different from the local oxygen profile over the lidar site or rocket trajectory. Species retrievals are important by its own right; the extent these improvements will impact kinetic temperature retrievals await for future study.

Based on the above discussions, it not only is difficult to make single profile or overpass comparisons, but it also makes better sense to compare means over an extended period of time, such as one month, between observations by lidar and TIMED/SABER. Monthly-mean temperature profiles obtained by two methods would yield a more reliable comparison on the one hand, and result in a climatological description of the thermal structure in the midlatitude mesopause region, on the other.

For TIMED/SABER temperature data, we use available data in a 60-day window to form the monthly mean, containing 30 days of the month in question and 15 days immediately before and 15 days data immediately after. The observed SABER temperatures within $\pm 5^o$ latitude of the lidar site (41^oN, 255^oE), i.e., in the latitude range of $36^oN - 46^oN$ (and the longitude range of $250^o - 260^o$ ($255^o \pm 5^o$), are included in the average for comparison. Since, by combining profiles from adjacent up and down scans, SABER produces one temperature profile every 53 seconds, there will be a number of over-passes in one local-time hour within the $\pm 5^o$ of coverage. For the lidar data, we use the hourly mean temperatures in the same 60-day window. However, for January and December, we use a 45-day window because there were no SABER temperature data in December, 2002, and no Lidar temperature data in January, 2004. For each local day with lidar data, there will be 1 to 8 hours of hourly-mean temperature profiles. In the 60-day window for the month of September, for example, we have 146 hourly-mean lidar temperature profiles, more-or-less evenly distributed among the 8 hours designated. During the same period, there were 103 2-min-mean over-pass SABER profiles distributed with more hours before the local midnight. Despite these differences in temporal resolution and in local time distribution between the two methods, the two instruments yield similar monthly-mean temperature profiles.

In order to make monthly mean temperature comparisons, the aliasing resulting from irregular local time coverage or data gaps should be avoided. In this analysis, we average all temperature profiles in the 8 hours at night (from LT=20:00 to LT=4:00) in the 60-day window. Though the lidar observations in 2003 contain data over a much longer period than the 8 hours chosen for this study, the SABER observations have missing measurements especially in hours near local noon, occasionally even in the entire 60-day window [Zhu et al., 2005]. Restricting the comparison to 8 hours centered at local midnight and using a 60-day window for monthly means, we are ensured of having data for most of the local time hours with both instruments.

Since the number of available temperature profiles in each hour within the 8-hour and 60-day window are not uniform, especially for the SABER observations, in order to reduce the effect of wave perturbations (mainly tidal effects), we use two steps for the calculation of the monthly-mean (nocturnal) temperatures. Using the available temperature profiles within the 60-day window, the hourly-averaged temperature profile for each local-time hour is first calculated. Then, we calculate the monthly mean temperature profile, $\mathrm{T}(\mathrm{z})$, by averaging the 8 hourly-averaged temperature profiles. The combined formula for calculating $\mathrm{T}(\mathrm{z})$ and the associated standard deviation, $\sigma_{\mathrm{Total}}(\mathrm{z})$, are given as follows:

$$\bar{T}(z)=\frac{\sum_{j=1}^{8}\bar{T}_j(z)}{8}=\frac{1}{8}\sum_{j=1}^{8}\left[\frac{\sum_{i=1}^{N_j}T_i(z)}{N_j}\right],$$

$$\sigma_{Total}(z)=\left\{\frac{1}{8}\sum_{j=1}^{8}\frac{\sum_{i=1}^{N_j}\left\{\left[T_i(z)-\bar{T}(z)\right]^2+\sigma_{m,i}^2(z)\right\}}{N_j}\right\}^{\frac{1}{2}}. \qquad (2)$$

Here, $\mathrm{N}_1,\mathrm{N}_2,\cdots,\mathrm{N}_8$, are the number of observations (within a 60-day window) in each of the 8 hours. $\overline{\mathrm{T}_1},\overline{\mathrm{T}_2},\cdots,\overline{\mathrm{T}_8}$, are the hourly-averaged temperatures for each individual hour. $\bar{\mathrm{T}}(\mathrm{z})$ and $\sigma_{\mathrm{Total}}(\mathrm{z})$ are, respectively, the monthly mean (nocturnal) temperature and associated standard deviation profiles; they are averages weighted by the number of available profiles within each hour as prescribed by (2). This weighted average ensures that at each altitude, z, the hourly-averaged temperature for each of the 8 hours makes an equal contribution to the final monthly mean temperature at that altitude, thus properly smoothing out the tidal perturbations within the 8 hours to the extent possible. For the monthly mean temperatures computed from the lidar data, there are two contributions to the standard deviations, $\sigma_{Total}(z)$. First, the standard deviation of the hourly-averaged temperatures, resulting from geophysical variability from one hour to the next contributes to about 10 K due mainly to tidal effects and day-to-day variability. Second, the measurement error due to photon noise for lidar and to uncertainties in retrieval parameters for SABER. For each lidar temperature, the measurement

uncertainty is altitude dependent and calculated from observed photon noise in individual altitude. Near the peak of the sodium layer (~91 km), the measurement uncertainty, $\sigma_{m,i}(z)$, is less than 1 K, and it is negligible. However, near the edges of the Na layer, it may be greater than 5 K; it then contributes significantly to $\sigma_{Total}(z)$ in (2). For SABER temperatures, though there is no measurement uncertainty provided in version 1.04 (level 2A), we set $\sigma_{m,i}(z)$ = 5 K in (2), since the SABER team has estimated a temperature error of ~ 4-5 K in the 80-100km region.

3. Comparison between the SABER and Liar observed temperatures

The monthly-mean (night-time) temperature profiles for the 12 months in 2003 were calculated from TIMED/SABER and Lidar data using (2). The results are shown in Figs.1 and 2. In these figures, the associated standard deviations, $\sigma_{Total}(z)$, are also given. The observed monthly-mean temperature profiles for the two techniques are seen to be in very good agreement in the altitude range from 85 km to about 100 km throughout the year. We note that in this altitude range, the standard deviations of both Lidar and SABER observations, which varied between 10 and 20 K, are also in agreement and they well track one another. The fact that both instruments not only measure the same monthly means, but also measure comparable variability, due mainly to tidal effects, further increases our confidence in both instruments. The standard deviations of the SABER observations gradually increase from about 10 K at 70 km to more than 25 K at 110 km due to geophysical variability. Because of the photon noise contribution, $\sigma_{m,i}(z)$, the standard deviations of lidar observations are somewhat larger than those of SABER's below 85 km and above 100 km. Above 105 km and below 83 km, the photon noise of the lidar observations may be excessive, and we use these altitudes as the upper and lower limits of the lidar temperatures as was done in the eight-year CSU lidar nocturnal temperature climatology [She et al., 2000]. In June and July, the Na abundance is ~4 times lower than the peak monthly-mean in November, therefore we set their upper limit to be 103 km.

Other than the 5 months between Sep and Jan, there exists a consistent difference between lidar and SABER observations between 83 and 85 km, with the lidar temperature being warmer. Near 83 km, the lidar monthly means for March, April and June are in fact beyond the range of standard deviation of SABER temperatures. This is likely due to the fact that at the bottom side of the sodium layer, the density of atomic Na is not only very low but also drops more rapidly than in the top side. In this case, the temperature ratio for the

determination of temperature has lower counts in the numerator, thus more susceptible to noise contamination, leading to a possible bias toward warmer temperature. The comparison between the rocket measurement and the SABER temperature in the polar region, on the other hand, indicates that the two observations are in good agreement below 85 km [Mertens, et al. 2004].

Above 100 km, though again within each other's error bars, the monthly means of lidar temperatures of April, June and July are cooler than the corresponding SABER temperatures, while in the months of October, November and December, the Lidar temperatures are warmer. This difference is most noticeable in June and July when the lidar data show cooler temperatures gradually starting at ~ 95 km and reaching ~10 K cooler at 103 km. One possible reason is that the model calculated densities of atomic oxygen in June and July may be too low, giving rise to warmer SABER temperatures. The reverse may be true in November. That the October lidar temperatures between 83 and 95 km are cooler than those of SABER's is also noted. Since the maximum difference of ~10 K in this case occurred at ~87 km, where the lidar signal is strong, we can not blame this discrepancy on photon noise. One possible explanation is that the distributions of data in the 60-day window for October monthly-means between the two instruments are quite different; the Lidar data consists of 60 hours of observation in October and 51 hours in September, while the SABER data consists of 20, 25, and 15 over-passes, respectively in September, October and November. As shown in Fig. 1, the October mean temperatures at 87 km are 201 K and 210 K for the lidar and SABER observations. This may be compared to 205 K in the 8-year climatology [She et al., 2000], which has an October monthly-mean temperature profile (not shown) resembles the SABER profile better.

From Figs. 1 and 2, we can see that there exist two temperature minima in many monthly-mean temperature profiles, noticeably in February, March, May and September. The mesopause altitudes of the two observations are in excellent agreement except in the summer season (See Table 1). From January to March in the winter state, the two observations show that the mesopause altitudes are at a high-level [She and von Zahn, 1998]. And the mesopause altitudes decrease from above 100 km in January to below 100 km in March. From September to December, the mesopause altitudes are in accord with each other, except in November when the difference is ~3 km. Since the SABER mesopause altitude in November is in better agreement with the value in the 8-year climatology (see Table 1), this difference may be the result of not having enough lidar data within the 60-day period, 60 hours of Lidar data as compared to 73 more evenly distributed SABER over–passes. The largest mesopause altitude difference between the two techniques occurs from April to August. In this period, the mesopause altitudes are at a low-level or in the summer state. The mesopause altitudes observed by the lidar are located at about 86 km, while the mesopause altitudes of SABER observation are at around 82-83 km. Unfortunately, due to the fact that the tidal influence on mesopause altitude can not be assessed easily, it is difficult to determine the uncertainty (standard deviation) of the mesopause

altitudes in the monthly mean temperature in this study.

The poor Na lidar signal below 85 km in the summer months and its associated possible higher temperature bias may be responsible for the lidar observed summer mesopause to be 3 - 4 km higher than the SABER observation. However, we note that the SABER summer mesoapuse in the polar region was also ~4 km lower when compared to the rocket FS measurements in July 2002 [Mertens et al., 2004], though it is in a different regime where there are strong horizontal gradients. At midlatitudes, the summer mesopause altitude has also been measured by Rayleigh lidar in Southern France based on data between 1984 and 1989 [Hauchecorn et al., 1991], which does not use ratio for retrieval and should not have temperature bias with lower signal; they reported the mesopause altitude to be between 84 and 87 km (vertical resolution 3 km) for the months of May, June, July and August. On the other hand, early satellite data from the Solar Mesosphere Explorer (SME) has tabulated global temperature profiles based on observations between 1982 and 1986 [Clancy and Rush, 1989]; their reported mesopause altitude for the 4 months in summer at 40^{o}N are consistent with the SABER's observation. The SABER summer mesopause altitude is also consistent with UARS/HRDI [Ortland et al., 1998] and with CRISTA [Grossmann et al., 2002] observations. Thus, whether there is discrepancy of 3-4 km in the midlatitude summer mesopause altitude between ground-based and satellite observations, and if so what is the cause behind this difference appear to be open questions. Further investigation in this connection is warranted.

It is comforting to note that observations by both satellite-borne and ground-based instruments show the two-level mesopause thermal structure with a winter and a summer mesopause altitude, in agreement with previous studies [von Zahn, et al., 1996; Yu and She, 1995; She and von Zahn, 1998]. And the times at which the mesoapuse altitude changed from the winter state (or high-level) to the summer state (or low-level) and from summer to winter are in excellent agreement between the two observations. Table 1 also gives the monthly mean mesopause altitutes from the eight-year climatology over Fort Collins [She, et al., 2000]. The table indicates that there is agreement between two instruments on the transition times between two mesopause states in 2003; they moved ahead one month and postponed one month as compared with the eight-year climatology. This is due to the year-to-year variability in the middle atmosphere.

4. Conclusion

In this paper, we have made comparisons of the 60-day window averaged nighttime temperature profiles observed by the Na Lidar at Colorado State University and the TIMED/SABER instrument over-passes of the lidar site. The comparison indicates that in the range from 85 km to about 100 km, the two observations agree to within each the error bars and the profile shapes generally are in excellent agreement. The main differences occur below 85 km over the entire year and above 100 km in the summer season (above 95 km for June and

July). There are at least two possible reasons for this. The first is that due to the low Na density, the accuracy of the lidar is low below 85 km and above 100 km. Another possible reason is that some chemical species, such as, atomic oxygen, and nighttime CO_2 concentrations used in the SABER retrieval of the temperature distribution is based on the TIMED-GCM modeling output, which may be different from reality. For example, above 100 km, if the density of atomic oxygen used in the inversion calculation is too low, the inverted temperature will be larger than it is [Mertens, et al., 2001], as in the case of June and July. And the satellite observations of the atomic oxygen indicate that there are large difference between the satellite observation and the model prediction [Grossmann, et al., 2000]. Therefore, the high precision temperature inversion needs high precision observations of the chemical species. Further improvement in satellite temperature remote sensing hinges on accurate, simultaneous observations of more chemical species, such as, concentration of O and nocturnal CO_2. Of course, it would be very helpful to have a quenching rate k_O known to be accurate [Mertens, et al., 2001]. The current SABER processing algorithm (v1.06) uses SABER retrieved atomic oxygen fed back into the temperature retrieval and once these data become available, this analysis should be repeated to assess the impact of better known oxygen density and quenching rate on kinetic temperature retrieval.

Comparisons of the two sets of observations further confirms the concept of the two-level mesopause with the months of transition between winter and summer states in agreement between the two data sets. The mesopause altitudes of the two observations are in excellent agreement except in the summer season, when the mesopause altitudes observed by SABER appear to be lower than the Lidar observation. Though Na lidar signal is weak below 85 km in summer, the same disagreements exist in the summer mesopause altitude measured by Rayleigh lidar. On the other hand, the SABER mesopause altitude at midlatitude agrees well with SME and other satellite data. Therefore, further investigation is warranted.

Acknowledgements

This research was supported by the National Science Foundation of China (40225011, 40336054) and National Research Project (G2000078407) and project of CAS (KZCX3-SW-217). This work was also supported in part by the International Collaboration Research Team Program of the Chinese Academy of Sciences. The work in Colorado State University is in part supported by National Aeronautics and Space Administration, under grant NAG5-10076 and National Science Foundation, under grant ATM-00-03171.

Reference

Apruzese, John P., Darrell F. Strobel, and Mark P. Schoeberl, Parameterization of IR cooling in a middle atmosphere dynamics model 2. Non-LTE radiative transfer and the globally averaged temperature of the mesosphere and lower thermosphere, Journal of Geophysical Research, 89, 4917-4926, 1984.

Clancy, R. and D. W. Rush, Climatology and trends of mesospheric (58 – 90 km) temperatures based upon 1982 – 1986 SME limb scattering profiles, J. Geophys. Res., 94, 3377-3393, 1989.

Fomichev, V. I., Kutepov A ,Akmaea and R A, Shved G M. Parameterization of the 15 μm CO_2 band cooling in the middle atmosphere (15-115 km). J. Atmos. Terr. Phys., 55, 7-18, 1993.

Fomichev, V. I., Ward W E, McLandress C. Implications of variations in the 15-μm CO_2 band cooling in the mesosphere and lower thermosphere associated with current climatologies of the atomic oxygen mixing ratio. J. Geophys. Res., 101, 4041-4055, 1996.

Fritts, D. C.; Williams, B. P.; She, C. Y.; Vance, J. D.; Rapp, M.; Lübken, F.-J.; Müllemann, A.; Schmidlin, F. J.; Goldberg, R. A., Observations of extreme temperature and wind gradients near the summer mesopause during the MaCWAVE/MIDAS rocket campaign, Geophys. Res. Lett., 31, CiteID L24S06, doi:10.1029/2003GL019389, 2004.

Grossmann, K. U.; Kaufmann, M.; Gerstner, E., A global measurement of lower thermosphere atomic oxygen densities, Geophysical Research Letters, 27, 1387-1390, 2000.

Grossmann, K. U., D. Offermann, O. Gusev, J. Oberheide, M. Riese, and R. Spang, The CRISTA-2 mission, J. Geophys. Res., 107(D23), 8173, doi:10.1029/2001JD000667, 2002.

Hauchecorne, A., M.-L. Chanin and P. Keckhut, Climatology and trends of the middle atmospheric temperature (33-87 km) as seen by Rayleigh lidar over the South of France, J. Geophys. Res., 96, 15297-15309, 1991.

Hecht, J. H., A. Z. Liu, R. L. Walterscheid, R. G. Roble, M. F. Larsen, and J. H. Clemmons, Airglow emissions and oxygen mixing ratios from the photometer experiment on the Turbulent Oxygen Mixing Experiment (TOMEX), Journal Of Geophysical Research, 109, D02S05, doi:10.1029/2002JD003035, 2004.

Howlett, L. C.; Baker, K. D.; Megill, L. R.; Shaw, A. W.; Pendleton, W. R.; Ulwick, J. C., Measurement of a structured profile of atomic oxygen in the mesosphere and lower thermosphere, Journal of Geophysical Research, 85, 1291-1296, 1980.

Iwagami, N.; Shibaki, T.; Suzuki, T.; Sekiguchi, H.; Takegawa, N.; Morrow, W. H., Rocket observations of atomic oxygen density and airglow emission rate in the WAVE2000 campaign, Journal of Atmospheric and Solar-Terrestrial Physics, 65, 1349-1360, 2003.

Kostov, V. S., On the location of a priori information to the solution of inverse problems of remote sensing of the non-LTE atmosphere in the infrared region by high-resolution spectral instruments, Advances in Space Research, 21, 405-408, 1998.

Lübken, F.-J., and U. von Zahn, Thermal structure of the mesopause region at polar latitudes, J. Geophys. Res., 96, 20841-20857, 1991.

Lübken, F.-J., A. Müllemann, First in situ temperature measurements in the summer mesosphere at very high latitudes (78°N), J. Geophys. Res., 108,D 8448, DOI 10.1029/2002JD002414, 2003.

Lübken, F.-J., Thermal structure of the arctic summer mesosphere, J. Geophys. Res., 104, 9135-9150, 1999.

Melo, S. M. L.; Takahashi, H.; Clemesha, B. R.; Batista, P. P.; Simonich, D. M., Atomic oxygen concentrations from rocket airglow observations in the equatorial region, Journal of Atmospheric and Terrestrial Physics, 58, 1935-1942, 1996.

Mertens Christopher J., Francis J. Schmidlin, Richard A. Goldberg, Ellis E. Remsberg, W. Dean Pesnell, James M. Russell III, Martin G.. Mlynczak, Manuel López-Puertas, Peter P. Wintersteiner, Richard H. Picard, Jeremy R. Winick, and Larry L. Gordley, SABER observations of mesospheric temperatures and comparisons with falling sphere measurements taken during the 2002 summer MaCWAVE campaign, *Geophys. Res. Lett.*, *31*, L03105, doi:10.1029/2003GL018605, 2004.

Mertens Christopher J., M Martin G. Mlynczak, Manuel López-Puertas, Peter P. Wintersteiner, R. H. Picard, Jeremy R.Winick, Larry L.Gordley, and James M.Russell III, Retrieval of mesospheric and lower thermospheric kinetic temperature from measurements of CO_2 15 μm Earth limb emission under non-LTE conditions, Geophys. Res. Lett. 28, 1391-1394, 2001.

Mertens Christopher J., Martin G. Mlynczak, Manuel López-Puertas, and Ellis E. Remsberg, Impact of non-LTE processes on middle atmospheric water vapor retrievals from simulated measurements of 6.8 mum Earth limb emission, Geophysical Research Letters, 29,D1288 DOI 10.1029/2001GL014590, 2002.

Mlynczak M G, Solomon S. A detailed evaluation of the heating efficiency in the middle atmosphere. J. Geophys. Res., 98, 10517-10541, 1993.

Mlynczak, Martin G., Daniel K. Zhou, Manuel Lopez-Puertas, Guillermo Zaragoza, and James M. Russell, Kinetic requirements for the measurement of mesospheric water vapor at 6.8 mum under non-LTE conditions, Geophysical Research Letters, 26, 63-66, 1999.

Russell, J. M. III, M. G. Mlynczak, L. L. Gordley, J. Tansock, and R. Esplin, An overview of the SABER experiment and preliminary calibration results, Proceedings of the SPIE, 44th Annual Meeting, Denver, Colorado, July 18-23, 3756, 277-288, 1999.

Ortland, D. A., P. B. Hays, W. R. Skinner, and J.-H. Yee, Remote sensing of mesospheric temperature and O2 (1S) band volume emission rates with the high-resolution Doppler imager, J. Geophys. Res,, 103, 1821-1835, 1998.

She, C. Y. and U. von Zahn, The concept of two-level mesopause: Support through new lidar observation, J. Geophys. Res., 103, 5855 - 5863, 1998.

She, C. Y., S. S. Chen, Z. L. Hu, J. Sherman, J. D. Vance, V. Vasoli, M. A. White, J. R. Yu, and D. A. Krueger, Eight-year climatology of nocturnal temperature and sodium density in the mesopause region (80 to 105 km) over Fort Collins, CO (41^{o}N, 105^{o}W), Geophys. Res. Lett., 27, 3289 - 3292, 2000.

She, C.-Y., Initial full-diurnal-cycle mesopause region lidar observations: Diurnal-means and tidal perturbations of temperature and winds over Fort Collins, CO (41N, 105W), PSMOS 2002, J. Atmo. Solar-Terr. Phys. 66, 663-674, 2004.

States, R. J.; Gardner, C. S., Structure of the mesospheric Na layer at 40°N latitude: Seasonal and diurnal variations, Journal of Geophysical Research, 104,11783-11798 , 1999.

von Zahn, U., J. Höffner, V. Eska, and M. Alpers, The mesopause altitude: Only two distinctive levels worldwide?, Geophys. Res. Lett. 23 , 3231-3234, 1996.

Yu, J. R., and C. Y. She, Climetology of a midlatitude mesopause mesopause region observed by a lidar at Fort Collins, Colorado (40.6^{o}N, 105^{o} W), J. Geophys. Res., 100, 7441-7452, 1995.

Zhou, D. K., M. G. Mlynczak, L M. López-Puertas, and G. Zaragoza, Evidence of non-LTE effects in mesospheric water vapor from spectrally-resolved emissions observed by CIRRIS-1A, Geophysical Research Letters, 26, 67-70 ,1999.

Zhu, Xun; Yee, Jeng-Hwa; Talaat, E. R.; Mlynczak, M.; Gordley, L.; Mertens, C.; Russell, J. M., III, An algorithm for extracting zonal mean and migrating tidal fields in the middle atmosphere from satellite measurements: Applications to TIMED/SABER–measured temperature and tidal modeling, J. Geophys. Res., 110, D02105, 10.1029/2004JD004996, 2005.

Table 1 Monthly nighttime averaged mesopause altitude (km) for Lidar and SABER observations.

Month	Jan.	Feb.	Mar.	Apl.	May	June	July	Aug.	Sep.	Oct.	Nov.	Dec.
Lidar*	102.5	101.5	97.5	86.5	86.0	86.0	86.0	85.5	99.5	100.5	98.0	101.5
SABER	102.0	101.0	98.0	83.0	82.0	82.0	84.0	82.0	99.0	101.0	101.0	101.0
Lidar**	102.5	102.5	101.5	100.0	87.5	85.5	86.5	99.5	100.5	100.5	101.0	102.0

* Mesopause altitude in 2003.

** Eight years climatology for the mesopause altitude [She, et al., 2000].

Figure captions:

Fig. 1 The monthly-mean nocturnal temperature profiles of lidar and SABER observations with standard deviation for the months of January through June in 2003.

Fig. 2 Same as Fig. 1, except for the months of July through Dec in 2003.

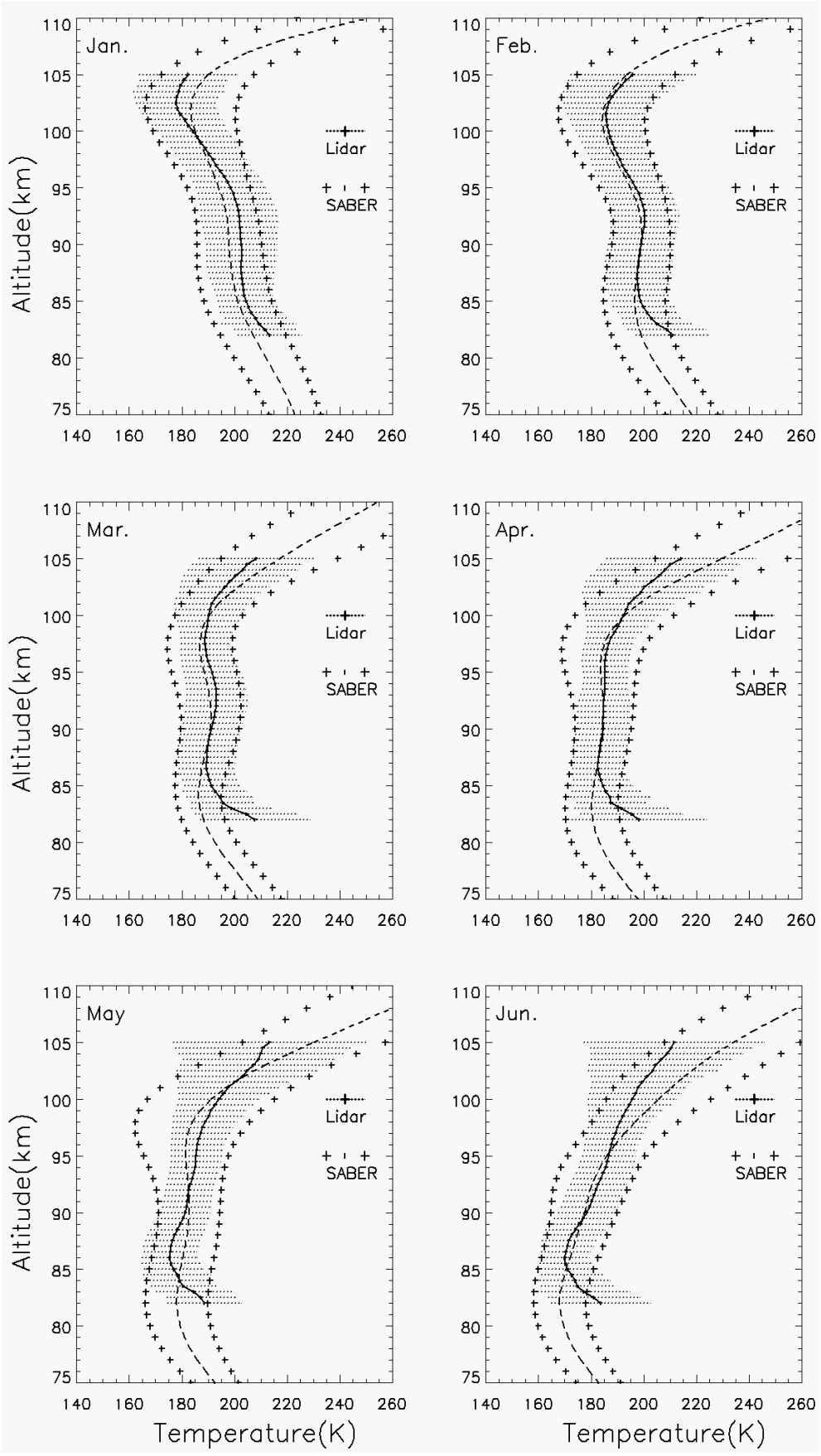
Jan.
Feb.
Mar.
Apr.
May
Jun.
Lidar
SABER
Altitude(km)
Temperature(K)
110
105
100
95
90
85
80
75
140
160
180
200
220
240
260

Fig 1

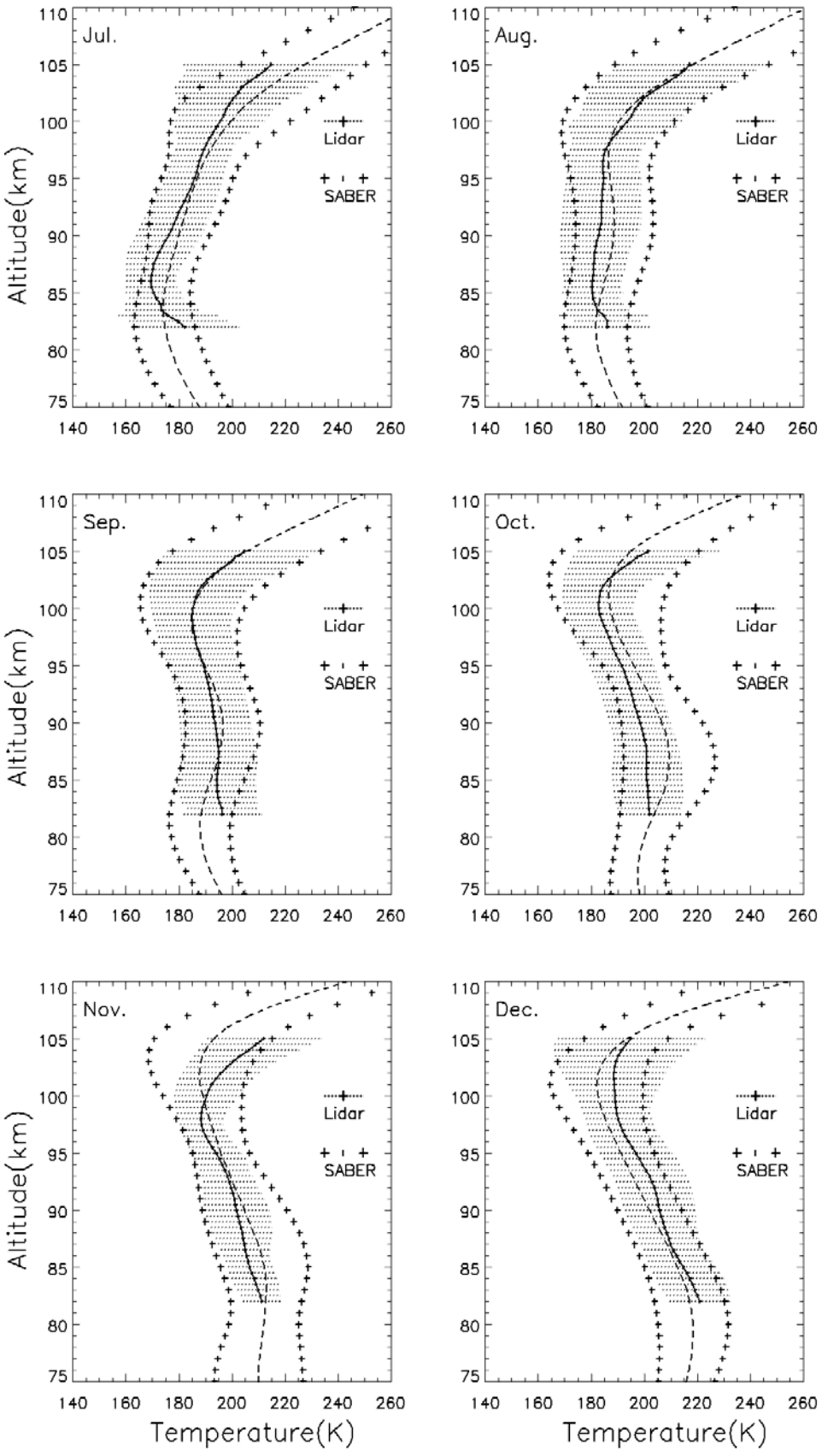
Jul.
Aug.
Sep.
Oct.
Nov.
Dec.
Lidar
SABER
Altitude(km)
Temperature(K)
110
105
100
95
90
85
80
75
140
160
180
200
220
240
260

Fig.2